# A complete MC optical photons tracking simulation of Plastic Scintillator Detectors for the next generation of satellite experiments

To cite this article: C. Altomare *et al* 2022 *J. Phys.: Conf. Ser.* **2374** 012050



Journal of Physics: Conference Series **2374** (2022) 012050 doi:10.1088/1742-6596/2374/1/012050

# A complete MC optical photons tracking simulation of Plastic Scintillator Detectors for the next generation of satellite experiments

**Altomare C.*** [1,2], **Alemanno F.** [3,4], **Barbato F.C.T.** [3,4], **Bernardini P.** [5,6], **Cattaneo P.W.** [7], **De Mitri I.** [3,4], **de Palma F.** [5,6], **Di Venere L.** [1,2], **Di Santo M.** [3,4], **Fusco P.** [1,2], **Gargano F.** [1], **Kyratzis D.** [3,4], **Loparco F.** [1,2], **Loporchio S.** [1], **Marsella G.** [8], **Mazziotta M.N.** [1], **Pantaleo F.R.** [1,2], **Parenti A.** [3,4], **Pillera R.** [1,2], **Rappoldi A.** [7], **Raselli G.L.** [7], **Rossella M.** [7], **Serini D.** [1], **Silveri L.** [3,4], **Surdo A.** [6], **for the HERD collaboration.**

[1] Istituto Nazionale di Fisica Nucleare - Sezione di Bari, Italy
[2] Dipartimento Interateneo di Fisica dell'Università e del Politecnico di Bari, Italy
[3] Gran Sasso Science Institute (GSSI), Via Iacobucci 2, I-67100 L'Aquila, Italy
[4] Istituto Nazionale di Fisica Nucleare (INFN)–Laboratori Nazionali del Gran Sasso, I-67100 Assergi, L'Aquila, Italy
[5] Dipartimento di Matematica e Fisica "E. De Giorgi", Università del Salento, I-73100, Lecce, Italy
[6] Istituto Nazionale di Fisica Nucleare (INFN)–Sezione di Lecce, I-73100 Lecce, Italy
[7] Istituto Nazionale di Fisica Nucleare (INFN)–Sezione di Pavia, Italy
[8] Dipartimento di Fisica e Chimica "E. Segrè", Università degli Studi di Palermo, Italy

E-mail: `corrado.altomare@ba.infn.it`

**Abstract.** Plastic scintillators are widely used for anti-coincidence systems and for the identification of charged cosmic-ray nuclei in satellite experiments. For this reason, a plastic scintillator detector (PSD) should have a high detection efficiency for charged cosmic rays and a very good capability of measuring charges. We implemented a full and customizable simulation tool to investigate the performance of a PSD coupled to Silicon Photomultipliers. The overall performance of the detector is studied by tracking optical photons produced inside the scintillator. The simulation will be used for the design of a PSD for future space experiments, such as HERD, AMEGO, e-Astrogam. In this work we investigated in detail the effect of Birks' saturation in the discrimination of charged ions up to iron nuclei. We will show the comparison between simulations and measurements conducted on prototype scintillator tiles.

## 1. Introduction

Satellite experiments aimed to the detection of gamma rays and/or charged cosmic rays often employ plastic scintillators to discriminate charged from neutral particles and to correctly identify the different species of cosmic-ray nuclei. A Plastic Scintillator Detector (PSDs) [1] needs to have a very high detection efficiency for charged cosmic rays, which represent the main background for the identification of gamma rays, and a very good capability of identifying the charged nuclei. Highly segmented PSDs are also required in order to reduce the false

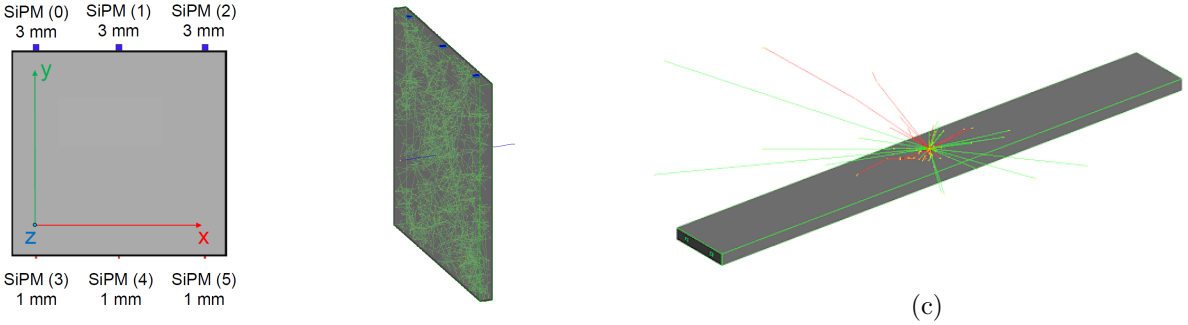


(a) (b) (c)

Figure 1: a) Geometry of the simulated scintillator tile with the SiPMs on the top and on the bottom faces; b) Display of a simulated event of a relativistic muon; the green line indicate the paths of optical photons in the tile; c) Other PSD geometry under test (bar option).

veto signals induced by back-splashes of secondary particles produced in the electromagnetic showers initiated by gamma rays entering in the detector. The optimization of the geometry is therefore essential to maximize the performance of a PSD. Next-generation space missions, such as HERD [2, 3], AMEGO [4], e-Astrogram [5] will likely employ silicon Photomultipliers (SiPMs) instead of classical photomultiplier tubes to read out the scintillation light, to exploit their smaller sizes, higher mechanical stability and lower power consumption.

## 2. Simulation results

We developed a fully customizable simulation code for organic scintillators based on `GEANT4` [6]. The code allowed to implement different geometries, detector read-outs, scintillating materials and different reflective wrappings. For the PSD segmentation two different geometries were under evaluation: the tile option (Fig.1a) and the bar option (Fig.1c). The latter is presented in this work, while the former is currently under test with the same Monte Carlo code. We simulated a plastic scintillator tile ($10 \times 10 \times 0.5$ cm$^3$), equipped with 3 "large" SiPMs ($3 \times 3 \times 0.5$ mm$^3$) coupled to one side of the tile and 3 "small" SiPMs ($1 \times 1 \times 0.5$ mm$^3$) coupled to the opposite side, see Fig.1a. The scintillating material chosen was the BC-404 [7] plastic scintillator and its scintillation yield was set to 10400 photons/MeV. The main feature of our simulation is the possibility to track all individual optical photons (a photon tracking example is shown in Fig.1b). Photon production can be due to two processes: the Cerenkov effect (depending on the material refractive index) and the scintillation process (ruled by the light yield of the material). Birks'law, which describes the dependence of the light yield on the energy loss, has been also implemented with the possibility to set the Birks'parameter.

### *2.1. Birks' law*

The Birks' saturation effect in plastic scintillator is limited to the region close to the primary energy deposit (scintillation "core"), while the response is still linear in the far region (scintillation "halo") [8]. The "halo" is mainly due to the $\delta$-ray electrons which deposits their energy far from the primary ion. We have simulated the SiPMs response to different beams of ions with increasing $Z$ from 1 (H) to 20 (Ca) and with a kinetic energy of 150 GeV/nucleon crossing the tile in its center, with normal incidence. For each set of simulations we have recorded the number of generated photons with respect to the total energy deposit.

The plot in Fig. 2a shows the mean number of generated photons as a function of the energy deposited by the primary particle. The energy deposited increases with $Z^2$ (Bethe energy loss formula [9]). The blue points from left to right corresponds to p, $He^{+2}$, $Li^{3+}$,

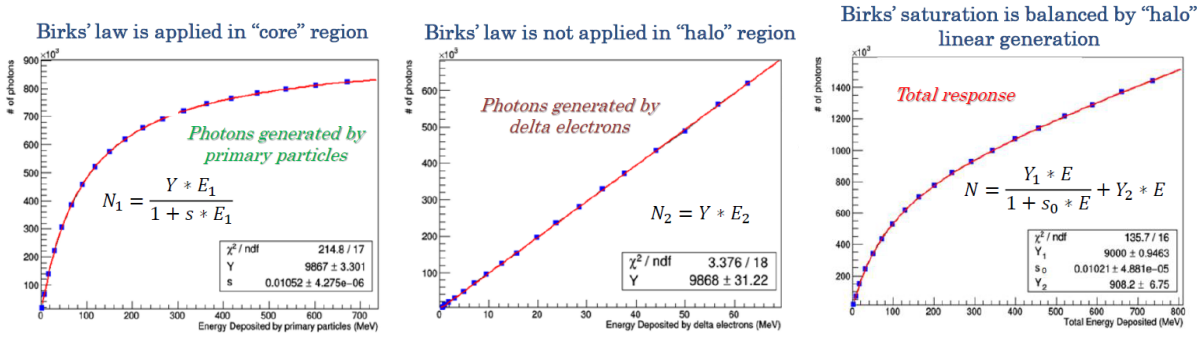


(a) (b) (c)

Figure 2: The plots blue points represents the mean number of photons produced as function of the average energy deposited for a set of 1000 simulations, were obtained simulating samples of different ions with 150 GeV/nucleon kinetic energy, crossing the tile in the central position (from left p, $He^{2+}$, $Li^{3+}$, ...). a) Energy deposited only by primary particles b) Energy deposited only by $\delta$-rays. c) Energy deposited by primary + $\delta$-rays.

etc... As shown in the plot, the behaviour of the photon production is affected by the saturation mechanism ("core scintillation"), and it is well described by Birk's equation [10]. However, in the simulation framework, it is possible to distinguish photons generated by primary particle from those generated in different processes. The plot Fig. 2b shows the mean number of photons produced by $\delta$-rays as a function of the average deposited energy. In this case, the number of $\delta$-electrons increases with the atomic number $Z$ of the primary particle, but the deposited energy per electron does not depend on $Z$ and the production of photons generated by $\delta$-rays is not affected by the Birks'saturation effect because $\delta$-rays lose their energy far away from the primary particle ("halo scintillation"). The total number of generated photons as a function of the average energy deposited is shown in Fig. 2c. We see that for low-Z nuclei (small energy depositions) the scintillator response is dominated by the photons generated by the primary particle, while for high-Z nuclei (large energy depositions) the contribution from delta rays becomes more relevant.

### *2.2. SiPM response*

We tested the response uniformity of light collection for three different species of relativistic ions (proton, carbon and iron) impinging on the tile. Fig.3a shows a scatter plot of the sum of photons collected by the "large" SiPMs versus the sum of those collected by the "small" ones as a function of the position of the primary particle in the tile. The tile has been segmented in squares of 1.11 cm side for proton, 1.25 cm side for carbon nuclei and 2 cm side for iron nuclei. To obtain more accurate results, some models of the SiPM response were implemented in the simulation. First of all, we assumed the photon detection efficiency of the AdvanSiD NUV SiPM [11] (45% sensitivity @420 nm). Then, we simulated cross talk effect using a model based on a compound Gaussian [12] and a cross-talk probability of the 30%. The cross-talk effect happens when a photon activates more than one cell in the SiPM cell array (normally 1 fired cell correspond to 1 photon), and this increases the number of detected photons.

We compared the predictions of our model with experimental data taken with a $^{90}$Sr source placed in different positions (1 cm step in x and y axis). The results are shown in Fig.3b. The differences in the number of detected photons are mainly due to the perfect reflectivity of the simulated wrapping. In the real case the wrapping can absorb or trap some photons, causing a reduction in the final number of detected photons.

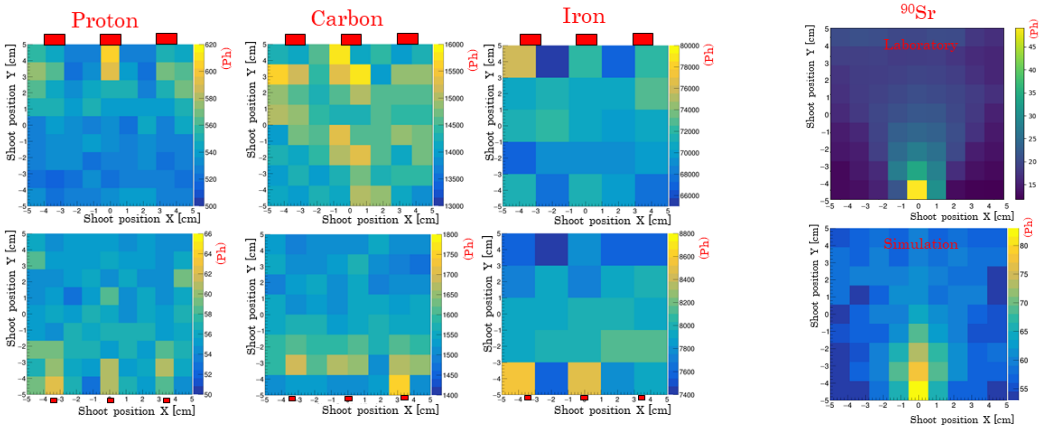


(a) (b)

Figure 3: a) Number of photons (Ph) entering in the three "large" SiPMs versus number of photons entering in the three "small" SiPMs for 3 different particles: protons, carbon and iron ions; b) Comparison of response uniformity between experimental data and simulated one using a source of $^{90}$Sr.

## Conclusion

We developed a dedicated simulation to study the properties of a plastic scintillator tile equipped with SiPMs for a PSD application in the next generation of space experiments. This simulation provides a good starting point to study the performance of a PSD coupled with SiPMs. In particular we have studied the response of a scintillator tile with different particles and sources in terms of the spatial uniformity response and collection time.

## References

[1] Altomare C, Luque P D L T, Di Venere L, Fusco P, Gargano F, Giordano F, Hu P, Loparco F, Loporchio S, Mazziotta M *et al.* 2020 *Nuclear Instruments and Methods in Physics Research Section A: Accelerators, Spectrometers, Detectors and Associated Equipment* **983** 164476
[2] Zhang S N, Adriani O, Albergo S, Ambrosi G, An Q, Azzarello P, Bai Y, Bao T, Bernardini P, Bertucci B *et al.* 2017 Introduction to the high energy cosmic-radiation detection (herd) facility onboard china's future space station *35th International Cosmic Ray Conference, ICRC 2017, 10 July 2017 through 20 July 2017* (Sissa Medialab Srl)
[3] Dong Y 2019 Overall status of the high energy cosmic radiation detection facility onboard the future china's space station *36th International Cosmic Ray Conference (ICRC2019)* vol 36 p 62
[4] Moiseev A, Team A *et al.* 2018 All-sky medium energy gamma-ray observatory (amego) *35th International Cosmic Ray Conference* vol 301 (SISSA Medialab) p 798
[5] De Angelis A, Tatischeff V, Tavani M, Oberlack U, Grenier I, Hanlon L, Walter R, Argan A, von Ballmoos P, Bulgarelli A *et al.* 2017 *Experimental Astronomy* **44** 25–82
[6] Agostinelli S, Allison J, Amako K a, Apostolakis J, Araujo H, Arce P, Asai M, Axen D, Banerjee S, Barrand G *et al.* 2003 *Nuclear instruments and methods in physics research section A: Accelerators, Spectrometers, Detectors and Associated Equipment* **506** 250–303
[7] Bc-404 URL `"https://www.crystals.saint-gobain.com/sites/imdf.crystals.com/files/documents/bc400-404-408-412-416-data-sheet.pdf"`
[8] Dwyer R and Zhou D 1985 *Nuclear Instruments and Methods in Physics Research Section A: Accelerators, Spectrometers, Detectors and Associated Equipment* **242** 171–176
[9] H Bethe J A 1953 *Experimental Nuclear Physics* **64** 253
[10] Birks J B 1951 *Proceedings of the Physical Society. Section A* **64** 874
[11] Advansid nuv sipm URL `"https://advansid.com/attachment/get/up_28_1432731773.pdf"`
[12] Vinogradov S 2012 *Nuclear Instruments and Methods in Physics Research Section A: Accelerators, Spectrometers, Detectors and Associated Equipment* **695** 247–251